JVSTB Journal of Vacuum Science & Technology B

Determination and analysis of minimum dose for achieving vertical sidewall in electron-beam lithography

Xinyu Zhao, Qing Dai, Soo-Young Lee, Jin Choi, Sang-Hee Lee, In-Kyun Shin, and Chan-Uk Jeon

Citation: Journal of Vacuum Science & Technology B **32**, 06F508 (2014); doi: 10.1116/1.4901013
View online: http://dx.doi.org/10.1116/1.4901013
View Table of Contents: http://scitation.aip.org/content/avs/journal/jvstb/32/6?ver=pdfcov
Published by the AVS: Science & Technology of Materials, Interfaces, and Processing

Determination and analysis of minimum dose for achieving vertical sidewall in electron-beam lithography

Xinyu Zhao, Qing Dai, and Soo-Young Lee[a)]
Department of Electrical and Computer Engineering, Auburn University, Auburn, Alabama 36849

Jin Choi, Sang-Hee Lee, In-Kyun Shin, and Chan-Uk Jeon
Mask Development Team, Samsung Electronics Co. Ltd., Hwasung, Gyeonggi-do 445-701, South Korea

(Received 29 June 2014; accepted 22 October 2014; published 6 November 2014)

Prior to carrying out the proximity effect correction by optimizing the spatial distribution of dose in electron beam lithography, one first needs to determine the minimum total dose required. A conventional method typically used to determine the minimum total dose is the trial-and-error approach, which can be unnecessarily costly and wasteful. In this paper, two new dose determination methods are described, which utilize the concept of a "critical path" without any proximity effect correction effort. Also, the dependency of the minimum total dose and dose distribution on the feature and lithographic parameters is investigated. The simulation results show that the proposed dose-determination methods can adaptively and efficiently determine the minimum total dose. Thus, they have the potential to provide a practical and effective alternative to the conventional trial-and-error approach. © *2014 American Vacuum Society*.
[http://dx.doi.org/10.1116/1.4901013]

I. INTRODUCTION

One of the major limiting factors in electron-beam (e-beam) lithography is the geometric distortion of written features due to electron scattering, i.e., the proximity effect, which limits the minimum feature size and the maximum pattern density that can be achieved. The importance of the proximity effect correction (PEC) has been well recognized and extensively investigated, and various effective methods have been developed.[1–6]

One of the effective PEC methods is to adjust the spatial dose distribution in order to achieve a resist profile close to the target profile. In our previous study,[6] the effectiveness of the conventional ("shape-V") and our proposed ("shape-M" and "shape-A") dose distribution types was studied to realize the target resist profile and, in particular, the most common sidewall shape of the vertical sidewall. The results showed that the shape-V dose distribution is not optimal for realizing a vertical sidewall in the resist profile for nanoscale features, especially when the total dose is to be minimized. However, our proposed shape-M and shape-A dose distributions significantly improved the correction results, which are much closer to the target resist profile in terms of the critical dimension (CD) error and sidewall shape (vertical) while minimizing the total dose.

In general, it is often desired to minimize the total dose because a lower total dose reduces the e-beam exposure time and the charging effect. In this study, the issue of determining the minimum total dose required for the PEC procedure is addressed. Conventional methods take an iterative trial-and-error approach, which determine the minimum total dose based on the resist profiles obtained through simulation or experiment. In each trial using a different total dose, PEC is carried out to adjust the spatial distribution of the total dose or an experiment is performed, and the CD error is measured from the simulated or experimental resist profile. This process is repeated with a number of total dose levels, and the minimum total dose is determined to be the lowest total dose resulting in the smallest CD error. One of the practical issues with such an approach is that in each trial an expensive simulation including the PEC or experiment must be carried out making the approach costly and wasteful.

In this study, to overcome the drawbacks of the conventional approach, two systematic methods of dose determination (iterative and noniterative) have been developed, which can adaptively determine the minimum total dose required for each type of dose distribution based on a given circuit pattern and substrate system setting. The proposed methods utilize the concept of a critical path in the dose determination to efficiently compute the developing time without any PEC effort. Also, the dependency of the minimum total dose and (optimal or best) spatial dose distribution on the feature and lithographic parameters is investigated.

The paper is organized as follows: the exposure model and development method are described in Sec. II. The dose distribution types are briefly reviewed in Sec. III. Details of the proposed dose determination methods are presented in Sec. IV. The feature and lithographic parameters considered in the analysis are described in Sec. V. Simulation results are discussed in Sec. VI, followed by a summary in Sec. VII.

II. SIMULATION

A. Exposure model

In a typical substrate system employed in this study, a resist layer with an initial thickness of H is on top of the substrate, as illustrated in Fig. 1 where the X–Y plane corresponds to the top surface of the resist and the resist depth is along the Z-dimension. The 3D point spread function (PSF) is denoted by $psf(x, y, z)$, which describes the exposure

[a)]Electronic mail: leesooy@eng.auburn.edu

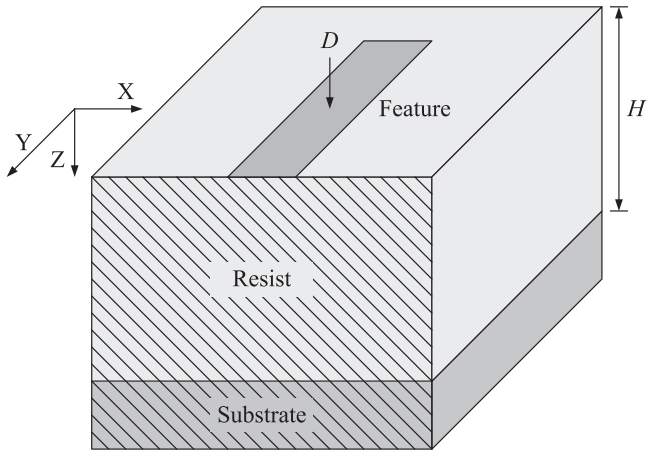

FIG. 1. Illustration of the substrate system.

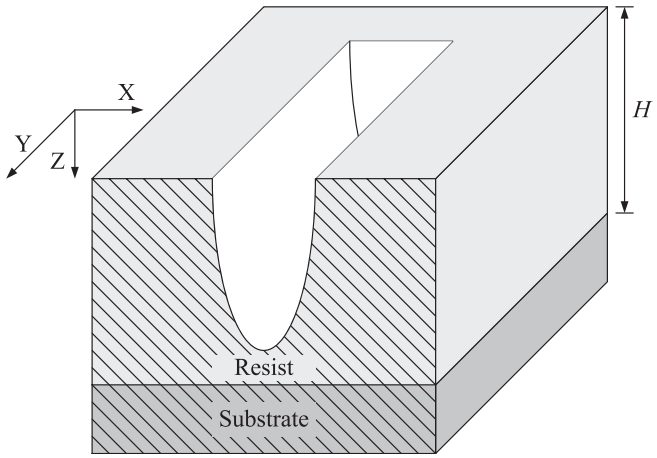

FIG. 2. Illustration of the remaining resist profile after the resist development process.

distribution in the resist when a point on the X–Y plane is exposed. Let $d(x, y, 0)$ represent the e-beam dose given to the point $(x, y, 0)$ on the surface of the resist for writing a circuit feature or pattern (Fig. 1). In the case of a uniform dose distribution, $d(x, y, 0)$ can be expressed as

$$d(x,y,0) = \begin{cases} D & \text{if } (x,y,0) \text{ is within the feature,} \\ 0 & \text{otherwise,} \end{cases} \quad (1)$$

where D is a constant dose.

Then, the 3D exposure distribution $e(x, y, z)$ in the resist is computed by

$$e(x,y,z) = \sum_x \sum_y d(x-x', y-y', 0) psf(x', y', z). \quad (2)$$

From Eq. (2), it can be seen that the exposure distribution at a certain depth z_0 can be computed by the 2D convolution between $d(x, y, 0)$ and $psf(x, y, z_0)$ in the corresponding plane $z = z_0$, i.e., $e(x, y, z)$ may be estimated layer by layer. Note that the PSF reflects all of the phenomena affecting energy deposition including the e-beam blur.

B. Resist development

Although the 3D exposure model provides complete information on how the electron energy is distributed in the resist, it does not directly depict the remaining resist profile after development, as illustrated in Fig. 2. Therefore, it is necessary to also take the resist development process into account to obtain a realistic result. The resist profile of a feature may be obtained through resist development simulation.

Before a resist development simulation is employed, the exposure at each point in the resist, $e(x, y, z)$, is converted into the corresponding developing rate, $r(x, y, z)$ through a nonlinear exposure-to-rate mapping function that is experimentally determined. A long line with a width of 100 nm is exposed with various dose levels (300 nm poly(methylmethacrylate) (PMMA) on Si, 50 keV). After resist development using methyl isobutyl ketone (MIBK) and isopropanol (IPA) (MIBK:IPA = 1:2), the center depth is measured in the cross-section of the remaining resist profile obtained for each dose level. Note that the resist is developed only vertically at the center of the line when the dose distribution within the line is uniform. The center depth is also obtained for each dose level through simulation based on our 3D exposure model. The mapping function employed in the simulation is modeled with two exponential (Gaussian) terms and a constant term. The coefficients in the mapping function are determined such that the difference between the depth measured in the experiment and the respective depth obtained via simulation is minimized. The mapping function used in this study (Fig. 3) is given as

$$\begin{aligned} r(x,y,z) &= F[e(x,y,z)] \\ &= 3700 \times 10^{-\left(\frac{e(x,y,z)-1.0\times10^{11}}{5.6\times10^{10}}\right)^2} - 80 \\ &\quad \times 10^{-\left(\frac{e(x,y,z)-9.0\times10^{9}}{9.0\times10^{9}}\right)^2} - 123, \end{aligned} \quad (3)$$

where the unit of $r(x, y, z)$ is nm/min and the unit of $e(x, y, z)$ is eV/μm^3.

A conventional cell-based resist development simulation such as the "cell removal method" [e.g., PEACE (Ref. 7)] is very time-consuming. In the cell removal method, the resist layer is partitioned into cubic cells and the resist development process is traced on a cell-by-cell basis, which requires

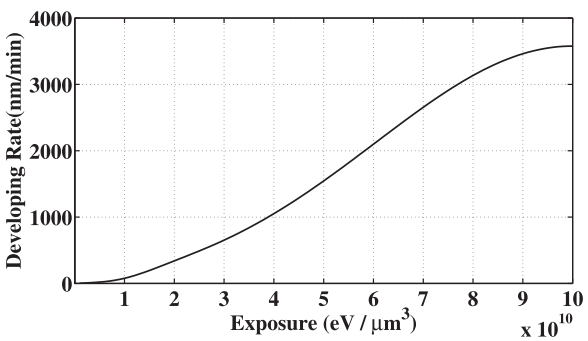

FIG. 3. Experimentally derived nonlinear exposure-to-rate mapping function.

incremental updating of cell states through a large number of iterations.

To overcome the drawbacks of the cell-based methods, a fast path-based simulation method was developed in our previous study.[8] In the path-based method, the resist development process is modeled by development paths starting from the resist surface toward the boundaries of the (remaining) resist profile. Each path consists of a vertical path segment (representing vertical development) and one or more lateral path segments (representing lateral development). All possible paths are traced without iterations, and those paths reaching the farthest points given a specified developing time determine the boundaries of the resist profile. It has been shown that this path-based method obtains resist profiles well matched with those obtained by the cell removal and fast marching methods and greatly reduces the simulation time, especially for features of regular shapes such as lines, rectangles, and circles.

It must be pointed out that the proposed methods for determining the minimum dose do not require any simulation of the resist development, though the path-based method is employed in analyzing the minimum dose by deriving the corresponding resist profile.

III. DOSE DISTRIBUTION TYPES

Suppose that a target written feature is specified by the corresponding resist profile (e.g., line widths at the top, middle and bottom layers) in 3D PEC. In our simulation model, the line is sufficiently long in the Y-dimension such that the dimensional variation along the Y-dimension may be ignored and therefore only the cross-section of the resist profile in the X–Z plane needs to be considered during correction (Fig. 2). Then, $e(x, y, z)$ and $r(x, y, z)$ can be replaced by $e(x, z)$ and $r(x, z)$, respectively.

To avoid a high complexity of the optimization procedure and to have sufficient spatial control of the dose distribution, the line feature is partitioned into five regions along its length dimension and a dose $d(i)$ $(i = 1, 2, 3, 4, 5)$ is determined for each region, as shown in Fig. 4.

In our previous study, new types of dose distributions that are effective in achieving a vertical sidewall with the total dose minimized were proposed with simulation results.[6] Their effectiveness was verified also through experiment.

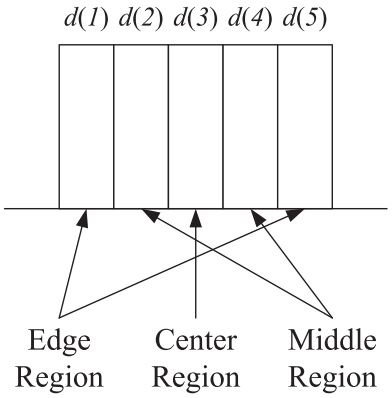

FIG. 4. Region-wise feature partitioning with a uniform dose distribution.

A. Shape-V dose distribution

A typical shape of spatial dose distribution over a line feature is the one where the dose is highest in the edge regions and gradually decreases toward the center region [to be referred to as shape-V: Fig. 5(a)]. This type of dose distribution is usually obtained by an exposure-based correction where a target 2D exposure distribution is specified (to be referred to as 2D exposure correction[3]). In the 2D exposure correction, the dose distribution is iteratively adjusted such that the error between the actual exposure distribution and the target one is minimized.

The shape-V dose distribution is widely employed and performs well when the feature size is relatively large. However, when the feature size decreases into the nanoscale, shape-V usually results in an undesired 3D resist profile in terms of CD error and sidewall shape, and requires a relatively higher total dose for full development. This is because the exposure variation along the resist depth dimension is not taken into account in the 2D model, though the resist profile depends upon the variation to a great extent. Furthermore, the 2D exposure correction does not consider the resist development process and therefore is likely to produce an unrealistic result.

B. Shape-M and shape-A dose distributions

To overcome the drawbacks of the 2D exposure correction, a resist-profile-based correction was developed along with a 3D model, referred to as 3D resist profile correction.[3] Unlike the above 2D exposure correction, this 3D correction incorporates the estimation of the remaining resist profile into the correction procedure and uses the resist profile to determine the dose distribution based on a 3D model. The overall correction procedure is similar to that of the 2D correction. However, the error, which is to be minimized by optimizing the dose distribution, is computed based on the estimated remaining resist profile rather than the exposure distribution.

Based on the 3D resist profile correction, two new types of dose distributions have been proposed and analyzed to achieve a target resist profile with the minimum total dose.[6] The two new types of dose distributions are one with the highest dose in the two middle regions [referred to as shape-M: Fig. 5(b)] and another with the highest dose in the center region and monotonically decreasing toward the edge regions [referred to as shape-A: Fig. 5(c)].

The feasibility of the two new types of dose distributions is due to the fact that the lateral development of the resist becomes comparable to the vertical development for nanoscale features, and the exposure varies along the resist depth dimension with high and low contrasts at the top and bottom layers of resist, respectively.[6,9] The new types of dose distributions take the exposure variation along the resist depth dimension (in addition to the lateral dimensions) into account, and balance the vertical and lateral developments of

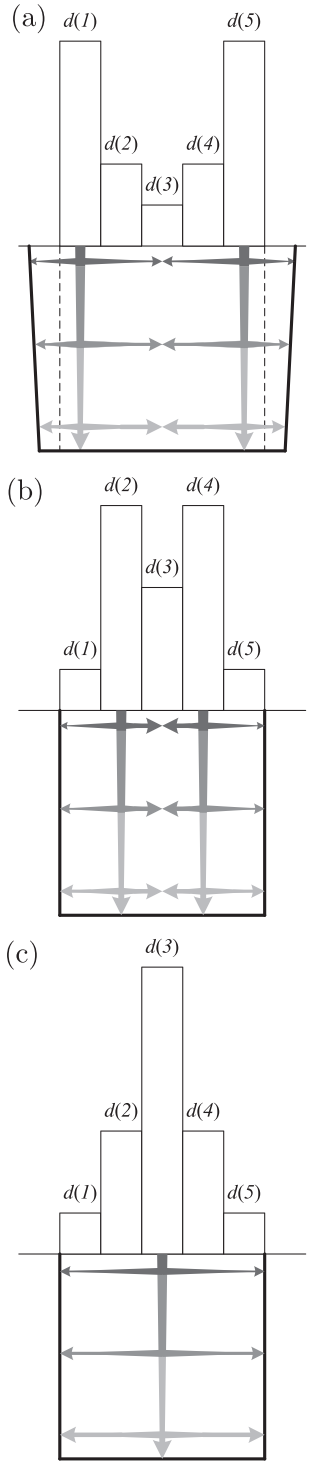

FIG. 5. Three types of dose distributions: (a) shape-V case, (b) shape-M case, and (c) shape-A case. The developing process and resulting resist profile are also illustrated in each type where a thicker arrow in the resist corresponds to a higher developing rate and a darker gray level indicates an earlier time in the developing process.

resist through the resist layers to achieve the target resist profile of a vertical sidewall (Fig. 5).

IV. DETERMINATION OF MINIMUM TOTAL DOSE

In this study, the characteristics of the above-mentioned dose distribution types (shape-V, shape-M, and shape-A) are further utilized to address the issue of effectively determining the minimum total dose. To avoid a time-consuming trial-and-error approach, two systematic methods are developed which determine the minimum total dose for each type of dose distribution based on a given circuit pattern and substrate system setting. A desired developing time is also given as an input to these methods.

A. Iterative method

The main idea of this iterative method is to start with a relatively low total dose. In each iteration, the total dose is increased by a small amount and the required developing time is examined. The iteration continues until the required developing time is smaller than the given developing time.

This process of determining the total dose is usually done prior to a PEC procedure, i.e., optimizing the spatial dose distribution. To avoid a high complexity of the required computation, a typical spatial distribution of dose for each type of dose distribution is selected and used in the determination of the minimum total dose. A region-wise dose ratio is defined as $q(1)$: $q(2)$: $q(3)$: $q(4)$: $q(5)$ where $q(i) = d(i)/min_j\{d(j)\}$. The region-wise dose ratios employed in this work are 4:2:1:2:4 for shape-V, 1:5:1:5:1 for shape-M, and 1:2:7:2:1 for shape-A. It needs to be pointed out that this dose ratio is only used to determine the minimum total dose and is not the final dose distribution (final dose ratio) that is derived by the dose optimization scheme presented earlier.[6]

The three (region-wise) base exposures $(e_i(x,z)\,|i = 1,2,3)$ are precalculated using the 3D exposure model (Sec. II A). Note that $e_i(x, z)$ is the exposure when a unit dose is given only to the ith and $(6 - i)$th regions, i.e., $d(i) = 1.0$ and $d(6 - i) = 1.0$ while the other regions are not exposed (Fig. 6).

Based on the dose ratio and the base exposures, the total exposure $e(x, z)$ can be computed by

$$e(x,z) = \frac{D \cdot \sum_{i=1}^{3} q(i) \cdot e_i(x,z)}{\sum_{j=1}^{5} q(j)}, \tag{4}$$

where D is the total dose given as $\sum_{i=1}^{5} d(i)$.

By converting the exposure into the developing rate through the mapping function $F[]$ [Eq. (3)], the required developing time is calculated along a specific critical path. The critical path is defined as the developing path in the resist development process, which must be checked to ensure that a target resist profile is achieved, as illustrated in Fig. 7. For example, in the case of shape-A, the critical path starts from the center region at the top layer of resist and goes vertically down to the bottom layer of resist. After reaching the bottom layer, it goes laterally toward the left or right and stops at the boundary between the exposed area and unexposed area (Fig. 7). The top layer of resist develops earlier than the bottom layer of resist. So, to achieve the vertical sidewall shape, after the developer reaches the bottom layer

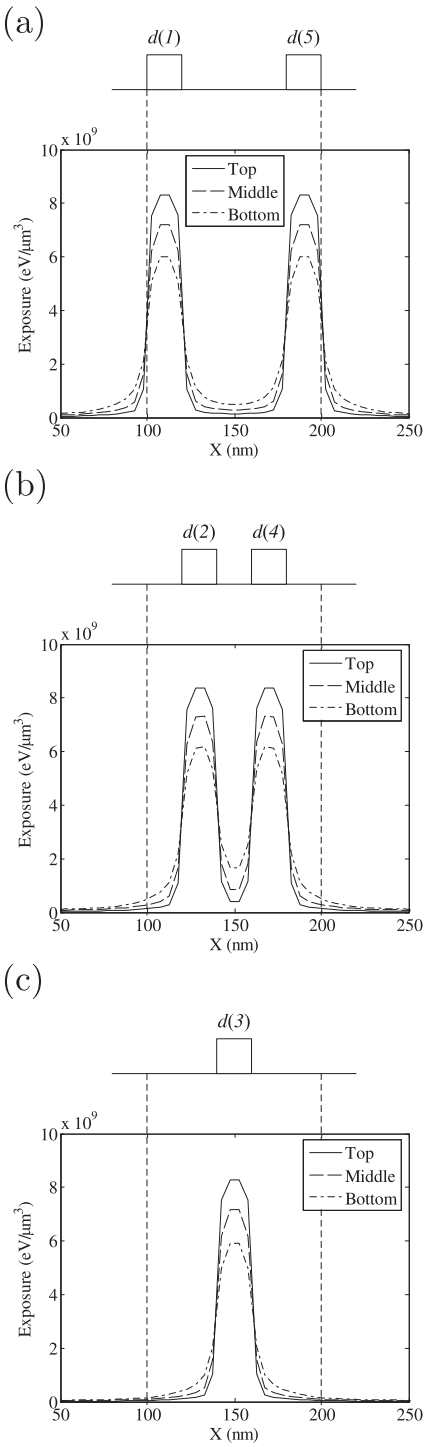

FIG. 6. Exposure distribution at the top, middle and bottom layers of resist when a unit dose is given to only (a) the two edge regions, (b) the two middle regions, and (c) the center region.

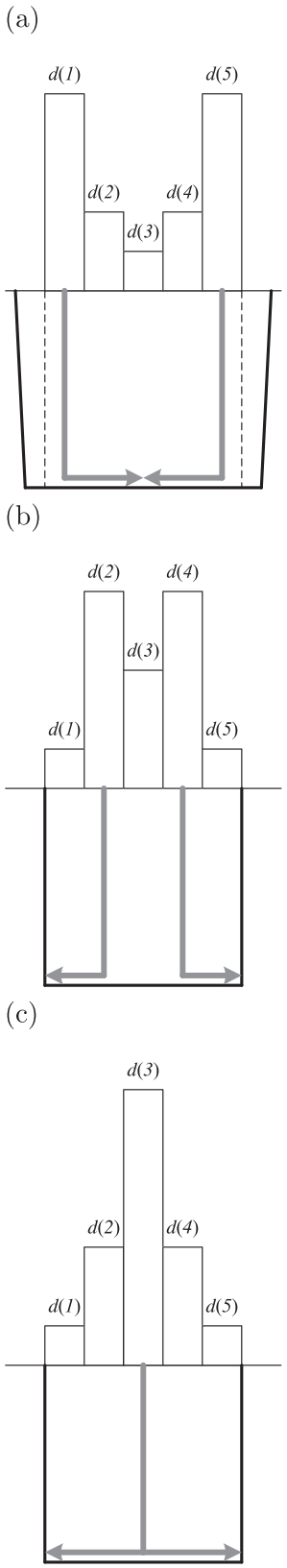

FIG. 7. Critical path: (a) shape-V case, (b) shape-M case, and (c) shape-A case.

of resist and develops laterally from the center region toward the edge region, it needs to catch up with the developing process of the top layer of resist at the boundaries of the feature (or slightly outside of the feature). Therefore, checking the critical path is sufficient to ensure that the required vertical sidewall shape is achieved. Note that the critical path is different for each different type of dose distribution.

The total dose D is updated through iteration such that the required developing time T spent on the critical path is smaller than the given developing time T_0 (the one specified for correction). The total dose which satisfies the developing

time condition is the minimum total dose for the given type of dose distribution.

The complete procedure of the iterative method to determine the minimum total dose given a developing time T_0 for a given type of dose distribution is provided below (also refer to the flowchart in Fig. 8).

Step 1: Calculate the three region-wise base exposures $e_i(x, z)$, and set an initial value D_0 for the total dose D. D_0 needs to be sufficiently lower than the dose level commonly used for the specified substrate system.

Step 2: Compute the total exposure $e(x, z)$ using the total dose D, the region-wise base exposures $e_i(x, z)$, and the preset region-wise dose ratio $q(i)$.

Step 3: Convert the total exposure $e(x, z)$ into the developing rate $r(x, z)$ through the mapping function $F[]$ defined in Eq. (3).

Step 4: Calculate the required developing time T along the critical path.

Step 5: Compare the required developing time T with the given developing time T_0 to obtain ΔT by $\Delta T = T - T_0$.

Step 6: If ΔT is negative and smaller than a certain threshold T_{th}, proceed to step 7. Otherwise, update the total dose D by $D = D + \Delta D$, where ΔD is qualitatively based on ΔT and go back to step 2.

Step 7: Output the current total dose D as the minimum total dose D_{min}.

This procedure may be repeated three times, once for each of the three dose distribution types. Then, the dose distribution type, which requires the lowest minimum total dose, can be selected as the best type of dose distribution. This best type of dose distribution with its minimum total dose, which can be used for our previously proposed dose optimization scheme,[6] thus makes the overall procedure more adaptive and efficient.

While this iterative method can determine the minimum total dose, it has some potential drawbacks. Depending on the difference between the initial total dose D_0 and the minimum total dose D_{min} and the dose increment per iteration, this iterative method can be time-consuming. Moreover, the accuracy of the result varies with the initial total dose and dose increment. To avoid these drawbacks, a noniterative method is also designed.

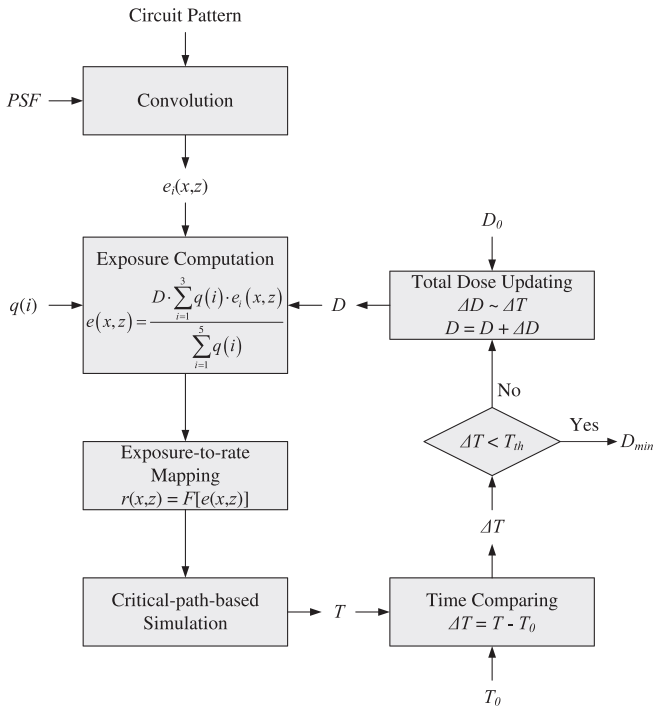

FIG. 8. Flowchart of the iterative method for a given dose distribution type where D_0 and D_{min} are the initial and minimum total doses, respectively.

B. Noniterative method

The main idea of this noniterative method is to get an initial estimate of the minimum total dose using the average exposure along the critical path, and then adjust the estimate by finding a correction factor considering the varying exposure along the critical path.

The average exposure $\bar{e}$ along the critical path is computed (Fig. 9) with an arbitrarily chosen total dose D_a, i.e.,

$$\bar{e} = \frac{1}{N}\sum_{i=1}^{N} e(i), \tag{5}$$

where N is the number of cells along the critical path and $e(i)$ represents the exposure in cell i.

Then, the average exposure $\bar{e}'$ converted from the average developing rate required is computed as

$$\bar{e}' = F^{-1}\left[\frac{L_{cp}}{T_0}\right], \tag{6}$$

where L_{cp} is the length of the critical path and $F^{-1}[]$ is the inverse mapping function which can convert the developing rate to the exposure [Eq. (3)].

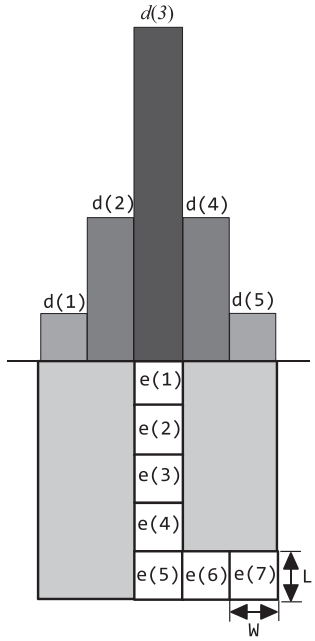

FIG. 9. Exposures of cells along the critical path (shape-A).

By comparing $\bar{e}$ and $\bar{e}'$, the minimum total dose can be estimated to be

$$D' = D_a \times \frac{\bar{e}'}{\bar{e}}. \tag{7}$$

When the range of exposure along the critical path is small or corresponds to the quasilinear portion of the exposure-to-rate mapping curve, D' can be close to the final minimum total dose or equivalently the one obtained by the iterative method. In such a case, the developing time estimated by the average exposure (or developing rate) would not be very different from that estimated by the point-by-point exposure. However, in general, the exposure varies significantly along the critical path, and therefore, the nonlinearity of exposure-to-rate conversion cannot be avoided. This leads to a substantial error in estimating the minimum total dose using the average exposure. Hence, D' is adjusted by finding a correction factor p satisfying

$$T_0 = \sum_{i=1}^{N} \frac{c(i)}{F[p \cdot E(i)]}, \tag{8}$$

where $c(i)$ is cell size (Fig. 9) and $E(i)$ is the exposure computed with the total dose of D'.

Since there is a linear relationship between the dose and exposure (with the region-wise dose ratio fixed), scaling the exposure with p is equivalent to scaling the dose with p. Therefore, p can be used to adjust D'. Note that the denominator of each term in the summation is the developing rate in the corresponding cell.

The exposure-to-rate mapping function $F[]$ is nonlinear. In solving Eq. (8) for p, $F[]$ is approximated to be piece-wise linear (Fig. 10) to avoid the complexity of a nonlinear equation. Note that $F[]$ is a smooth and monotonic function, and therefore, the linearization leads to a small error. The linearization is done such that the mean-square error is minimized.

Then, the developing rate can be computed by

$$r(i) = k_j \cdot e(i) + b_j \quad \text{if } e(i) \text{ is in the } j\text{th linear segment of } F[], \tag{9}$$

where k_j and b_j are the slope and y-intercept of the jth linear segment of $F[]$, respectively.

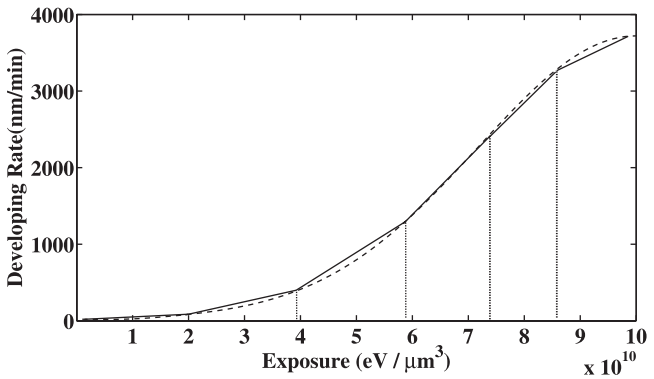

FIG. 10. Nonlinear mapping function (dashed curve) is approximated to be piece-wise linear (solid line segments).

After finding p, the minimum total dose D_{min} is computed as

$$D_{min} = p \cdot D'. \tag{10}$$

The complete procedure of the noniterative method to determine the minimum total dose, given a developing time T_0, for a given type of dose distribution is provided below:

Step 1: Compute the total exposure $e(x, z)$ using the total dose D_a, region-wise base exposures $e_i(x, z)$, and the preset region-wise dose ratio for the given type of dose distribution.

Step 2: Compute the average exposure $\bar{e}$ along the critical path.

Step 3: Estimate the minimum total dose by comparing $\bar{e}$ and $\bar{e}'$ [Eq. (7)].

Step 4: Adjust the estimated minimum total dose D' by finding a correction factor p satisfying Eq. (8).

Step 6: Compute the minimum total dose D_{min} to be $p \cdot D'$.

It should be clear that this noniterative method requires only the two steps of the initial estimation and adjustment, which is much less time-consuming than the iterative method. Also, the minimum total dose derived by the noniterative method is not affected by the initial guess of dose, D_0, and the dose increment step in the iterative method, and therefore is more accurate.

V. DEPENDENCY OF DOSE DISTRIBUTION ON FEATURE AND LITHOGRAPHIC PARAMETERS

After the minimum total dose and the best type of dose distribution are determined, a PEC procedure can be employed to optimize the (spatial) dose distribution. The dependency of dose distribution on a variety of parameters (feature and lithographic parameters) has been analyzed by considering the region-wise dose contrast for each type of dose distribution. The region-wise dose contrast is defined as the ratio of the highest dose to the lowest dose of all of the regions of a feature after correction; i.e., $d(1)/d(3)$ for the shape-V case, $d(2)/d(3)$ for the shape-M case, and $d(3)/d(1)$ for the shape-A case. These specific ratios play the most critical role in determining the resist profile. For example, in the case of shape-A, the rate of vertical development in the center of the feature most depends on $d(3)$, and that of lateral development in the edge region on $d(1)$ [and $d(5)$]. Therefore, the ratio of $d(3)/d(1)$ may be used to quantify the effect of dose distribution on the remaining resist profile for shape-A.

The parameters considered are listed below:

(1) Feature size and resist thickness, which determine the aspect ratio.
(2) Feature density, which affects the background exposure level in a pattern.
(3) Beam energy and beam diameter, which affect the intensity and range of the proximity effect.
(4) Total dose, which affects the average exposure level in the resist.
(5) Developing time, which affects the resist development process.

(6) Mapping function, which affects the contrast of the developing rates between the exposed area and the unexposed area.

VI. RESULTS AND DISCUSSION

A. Dose determination

The effectiveness of the proposed dose determination methods has been analyzed for a single line feature. However, they must be applicable to a pattern of multiple features by taking the background exposure into account. The PSFs used in the simulation are generated by a Monte Carlo simulation method, SEEL.[10] The substrate systems employed in the simulation are composed of PMMA on Si where three different resist thicknesses of 100, 300, and 500 nm, are considered with the three different beam energies of 20, 50, and 100 keV. Two different widths of a single-line feature of 50 and 100 nm are considered for performance analysis, and the length of the line is fixed at 3 μm. These different substrate systems along with the three different beam energies and two different feature sizes should provide a variety of combinations so that the proposed methods can be thoroughly tested.

In Table I, the best dose distribution types with the minimum total dose are determined under a variety of conditions using the proposed methods (Sec. IV). The results show that the minimum total dose obtained by the noniterative method is very close to that obtained by the iterative method in all cases, and the two methods agreed on the best type of dose distribution. It can be seen that the minimum total dose tends to be lower for a thinner resist, a lower beam energy, or a smaller feature size. In a thinner resist, the exposure level decreases less from the top layer to the bottom layer. For a lower beam energy, more beam energy is deposited in the resist. For a smaller feature size, the area dose required may be higher than for a larger feature, but the total dose is usually lower. Also, shape-M and shape-A dose distributions outperform the conventional shape-V dose distribution in almost all cases. The shape-M dose distribution has the best result when the aspect ratio is small, e.g., 1:1, but as the aspect ratio increases, the shape-A dose distribution tends to be the best one.

In Table II, the two methods are also compared in terms of computation time measured using an Intel Core *i*7–3615QM with a core clock of 2.3 GHz. The speed-up is defined as the ratio of the computation time required by the iterative method T_i to that by the noniterative method T_n, i.e.,

$$S_p = \frac{T_i}{T_n}. \tag{11}$$

The results show that the computation time for the iterative method increases when the initial dose is much lower than the final value. On the other hand, the computation time for the noniterative method is almost constant. Note that the computation time for the noniterative method is slightly larger for a wider feature size. This is due to the fact that the degree of the polynomial in Eq. (8) increases with increasing feature size since the width of the cell is fixed.

B. Dependency of dose distribution

The parameters considered are feature size (100/50 nm), feature density (0%, i.e., Isolated Feature/50%), resist thickness (100/300/500 nm), beam energy (50/20 keV), beam diameter (5/10 nm), total dose (220/250/280 μC/cm^2), developing time (36/40/45 s), and mapping function (low contrast/high contrast). The default setting consists of a feature size of 100 nm, a feature density of 0% (isolated feature), a resist of 300 nm PMMA, a beam energy of 50 keV, a beam diameter of 5 nm, an average dose of 250 μC/cm^2, a developing time of 40 s, and a low contrast mapping function.

To effectively analyze how the region-wise dose contrast is affected by the above parameters, each of them is changed individually while all of the others are held constant and fixed at the values in the default setting. The results are provided in Tables III, IV, and V.

TABLE I. Minimum total dose and best type of dose distribution.

Feature size (nm)	PMMA thickness (nm)	Beam energy (keV)	Beam diameter (nm)	Minimum dose required (μC/cm^2)						Best type
				Iterative			Non-iterative			
				Shape-V	Shape-M	Shape-A	Shape-V	Shape-M	Shape-A	
50	100	50	5	127	106	100	134	110	104	Shape-A
50	300	50	5	282	248	205	278	227	194	Shape-A
50	500	50	5	523	453	352	539	448	373	Shape-A
100	100	50	5	141	122	147	149	120	151	Shape-M
100	300	50	5	261	232	227	258	225	220	Shape-A
100	500	50	5	437	369	318	435	372	321	Shape-A
300	100	50	5	230	242	290	234	240	295	Shape-V
300	300	50	5	336	326	372	334	319	366	Shape-M
300	500	50	5	462	417	478	459	414	470	Shape-M
100	500	20	5	241	199	169	234	183	161	Shape-A
100	500	50	5	437	369	318	437	360	314	Shape-A
100	500	100	5	697	582	715	698	560	708	Shape-M

TABLE II. Computation times of the iterative and noniterative methods.

Dose distribution type	Feature size (nm)	PMMA thickness (nm)	Beam energy (keV)	Developing time (s)	Initial dose (μC/cm^2)	Computation time		Speed-up
						Iterative (s)	Non-iterative (s)	
Shape-V	100	100	50	30	100	3.59	0.01	359
Shape-M	100	100	50	30	100	3.14	0.01	314
Shape-A	100	100	50	30	100	3.71	0.01	371
Shape-V	100	300	50	30	100	7.25	0.01	725
Shape-M	100	300	50	30	100	6.32	0.01	632
Shape-A	100	300	50	30	100	6.12	0.01	612
Shape-V	50	300	50	30	100	7.52	0.007	1074
Shape-M	50	300	50	30	100	6.59	0.007	941
Shape-A	50	300	50	30	100	5.26	0.007	751
Shape-V	100	500	100	30	10	20.21	0.01	2021
Shape-M	100	500	100	30	10	16.84	0.01	1684
Shape-A	100	500	100	30	10	20.90	0.01	2090
Shape-V	100	500	100	15	10	28.36	0.01	2836
Shape-M	100	500	100	15	10	24.28	0.01	2428
Shape-A	100	500	100	15	10	29.79	0.01	2979

These tables show that a higher contrast dose distribution is usually obtained for a smaller feature size, a larger feature density, a thicker resist, a lower beam energy, a larger beam diameter, a lower total dose, a shorter developing time, or a lower contrast mapping function, respectively. For a smaller feature size, the path for the lateral development of the bottom layer of resist to catch up with that of the top layer of resist is shorter. For a larger feature density, the background exposure is higher. For a thicker resist, the exposure variation along the resist depth dimension is larger. For a lower beam energy or a larger beam diameter, the proximity effect is greater. For a lower total dose or a shorter developing time, the time for the lateral development of the bottom layer of resist to catch up with that of the top layer of resist is less. For a lower contrast mapping function, the contrast of developing rates between the exposed area and the unexposed area is lower. Therefore, a higher contrast dose distribution can compensate for these effects and provide a better correction quality.

VII. SUMMARY

In this study, two dose determination methods have been developed that use the concept of a critical path. The two methods can adaptively determine the best type of dose distribution and the minimum total dose based on a given circuit pattern and substrate system setting. Through extensive simulations, the effectiveness of the two methods has been verified. The results also show that the

TABLE III. Region-wise dose contrast: Shape-V dose distribution.

Feature size (nm)	Feature density (%)	Resist thickness (nm)	Beam energy (keV)	Beam diameter (nm)	Total dose (μC/cm^2)	Developing time (s)	Mapping function contrast	Dose contrast
100	0	300	50	5	250	40	Low	3.32
50	0	300	50	5	250	40	Low	6.70
100	0	300	50	5	250	40	Low	3.32
100	50	300	50	5	250	40	Low	400.2
100	0	100	50	5	250	40	Low	1.11
100	0	300	50	5	250	40	Low	3.32
100	0	500	50	5	250	40	Low	40.9
100	0	300	50	5	250	40	Low	3.32
100	0	300	20	5	250	40	Low	40.6
100	0	300	50	5	250	40	Low	3.32
100	0	300	50	10	250	40	Low	6.06
100	0	300	50	5	220	40	Low	8.18
100	0	300	50	5	250	40	Low	3.32
100	0	300	50	5	280	40	Low	1.65
100	0	300	50	5	250	36	Low	6.70
100	0	300	50	5	250	40	Low	3.32
100	0	300	50	5	250	45	Low	1.82
100	0	300	50	5	250	40	Low	3.32
100	0	300	50	5	250	40	High	2.23

TABLE IV. Region-wise dose contrast: Shape-M dose distribution.

Feature size (nm)	Feature density (%)	Resist thickness (nm)	Beam energy (keV)	Beam diameter (nm)	Total dose (μC/cm^2)	Developing time (s)	Mapping function contrast	Dose contrast
100	0	300	50	5	250	40	Low	29.2
50	0	300	50	5	250	40	Low	54.8
100	0	300	50	5	250	40	Low	29.2
100	50	300	50	5	250	40	Low	332.1
100	0	100	50	5	250	40	Low	15.5
100	0	300	50	5	250	40	Low	29.2
100	0	500	50	5	250	40	Low	41.7
100	0	300	50	5	250	40	Low	29.2
100	0	300	20	5	250	40	Low	126.9
100	0	300	50	5	250	40	Low	29.2
100	0	300	50	10	250	40	Low	33.1
100	0	300	50	5	220	40	Low	33.2
100	0	300	50	5	250	40	Low	29.2
100	0	300	50	5	280	40	Low	27.2
100	0	300	50	5	250	36	Low	30.0
100	0	300	50	5	250	40	Low	29.2
100	0	300	50	5	250	45	Low	20.1
100	0	300	50	5	250	40	Low	29.2
100	0	300	50	5	250	40	High	20.1

noniterative method is more efficient than the iterative method, especially when the initial dose used for the iterative method is much lower than the final value. The dependency of dose distribution on feature and lithographic parameters has also been analyzed by considering the region-wise dose contrast of each type of dose distribution. Simulation results under a variety of system parameters are provided. A higher dose contrast is usually obtained for a smaller feature size, a larger feature density, a thicker resist, a lower beam energy, a larger beam diameter, a lower total dose, a shorter developing time, or a lower contrast mapping function.

The proposed methods estimate the minimum total dose with a typical region-wise dose ratio fixed for each type of dose distribution. This allows one to exploit the linear relationship between the total dose and spatial exposure distribution and also to carry out the estimation prior to a PEC procedure. Also, the computational complexity can be kept low. When the final region-wise dose ratio after the PEC is different from the typical ratio, there can be an error in the

TABLE V. Region-wise dose contrast: Shape-A dose distribution.

Feature size (nm)	Feature density (%)	Resist thickness (nm)	Beam energy (keV)	Beam diameter (nm)	Total dose (μC/cm^2)	Developing time (s)	Mapping function contrast	Dose contrast
100	0	300	50	5	250	40	Low	20.1
50	0	300	50	5	250	40	Low	35.9
100	0	300	50	5	250	40	Low	20.1
100	50	300	50	5	250	40	Low	495.6
100	0	100	50	5	250	40	Low	16.5
100	0	300	50	5	250	40	Low	20.1
100	0	500	50	5	250	40	Low	72.1
100	0	300	50	5	250	40	low	20.1
100	0	300	20	5	250	40	low	30.0
100	0	300	50	5	250	40	low	20.1
100	0	300	50	10	250	40	Low	22.3
100	0	300	50	5	220	40	Low	24.6
100	0	300	50	5	250	40	Low	20.1
100	0	300	50	5	280	40	Low	18.2
100	0	300	50	5	250	36	Low	22.3
100	0	300	50	5	250	40	Low	20.1
100	0	300	50	5	250	45	Low	12.2
100	0	300	50	5	250	40	Low	20.1
100	0	300	50	5	250	40	High	10.0

minimum total dose derived by the methods, though the error would not be significant. To avoid any potential error in the minimum total dose, one may allow the region-wise dose ratio to vary during the estimation of the minimum total dose. However, this would increase the computation required for the estimation greatly such that any potential improvement in accuracy may not be well justified.

ACKNOWLEDGMENT

This work was supported by a research grant from Samsung Electronics Co., Ltd.

[1]M. Osawa, K. Ogino, H. Hoshino, Y. Machida, and H. Arimoto, J. Vac. Sci. Technol., B **22**, 2923 (2004).
[2]R. Murali, D. K. Brown, K. P. Martin, and J. D. Meindl, J. Vac. Sci. Technol., B **24**, 2936 (2006).
[3]S.-Y. Lee and K. Anbumony, J. Vac. Sci. Technol., B **25**, 2008 (2007).
[4]K. Ogino, H. Hoshino, and Y. Machida, J. Vac. Sci. Technol., B **26**, 2032 (2008).
[5]N. Unal, D. Mahalu, O. Raslin, D. Ritter, C. Sambale, and U. Hofmann, Microelectron. Eng. **87**, 940 (2010).
[6]Q. Dai, S.-Y. Lee, S.-H. Lee, B.-G. Kim, and H.-K. Cho, J. Vac. Sci. Technol., B **30**, 06F307 (2012).
[7]Y. Hirai, S. Tomida, K. Ikeda, M. Sasago, M. Endo, S. Hayama, and N. Nomura, IEEE Trans. Comput.-Aided Des. **10**, 802 (1991).
[8]Q. Dai, R. Guo, S.-Y. Lee, J. Choi, S.-H. Lee, I.-K. Shin, C.-U. Jeon, B.-G. Kim, and H.-K. Cho, Microelectron. Eng. **127**, 86 (2014).
[9]Q. Dai, S.-Y. Lee, S.-H. Lee, B.-G. Kim, and H.-K. Cho, Microelectron. Eng. **88**, 902 (2011).
[10]S. Johnson, "Simulation of electron scattering in complex nanostructures: Lithography, metrology, and characterization," Ph.D. dissertation (Cornell University, Ithaca, New York, 1992).